

## Supporting Information

# Simultaneous Activity and Surface Area Measurements on Single Mesoporous Nanoparticle Aggregates

*Xue Jiao<sup>a</sup>, Christopher Batchelor-McAuley<sup>a</sup>, Neil P. Young<sup>b</sup>, and Richard G. Compton<sup>a\*</sup>*

a. Department of Chemistry, Physical and Theoretical Chemistry Laboratory, University of  
Oxford, South Parks Road, Oxford OX1 3QZ, United Kingdom

b. Department of Materials, University of Oxford, Parks Road, Oxford OX1 3PH, United  
Kingdom

## Contents

S1: Experimental Section	S-3
S2: TEM and UV-Vis Characterisation	S-4
S3: Underpotential Hydrogen Deposition ( $H_{\text{upd}}$ ) Reduction	S-6
S4: Underpotential Hydrogen Deposition ( $H_{\text{upd}}$ ) Oxidation	S-7
S5: Mesoporous Platinum Nanoparticle Electroactive Surface Area Measurements	S-9
S6: Hydrogen Evolution Reaction (HER) under Hydrogen or Nitrogen Condition	S-10
S7: Current Density of Hydrogen Evolution Reaction (HER) on Platinum Bulk	S-12
Reference	S-14

## S1: Experimental Section

### 1.1 Chemicals

Hydrogen ( $\geq 99.98\%$  H<sub>2</sub>) was supplied from BOC, Surrey, U.K. Potassium nitrate ( $\geq 99.0\%$ , KNO<sub>3</sub>), Potassium hydroxide were obtained from Fisher Scientific, Loughborough, U.K. Citrate-capped mesoporous platinum nanoparticles (mesoporous PtNPs) were provided by nanoComposix, San Diego, CA, U.S.A., with a reported diameter 50 nm and concentration  $3.3 \times 10^{13}$  particles L<sup>-1</sup>. All solutions were prepared with ultrapure water from Millipore, with a resistivity of not less than 18.2 MΩ cm at 298 K.

### 1.2 Electrochemistry

All ensemble and nano-impact electrochemical experiments were performed on a three-electrode system in a Faraday cage. The working electrode was a gold microdisc electrode of diameter 10 μm from ALS, Tokyo, Japan, and the electrode was polished with alumina powders from Buehler, Lake Bluff, IL, U.S.A., in a size sequence of 1.0, 0.3, and 0.05 μm. A leakless silver/silver chloride electrode [Ag/AgCl, 1.0 M KCl] from Cypress Systems, Lawrence, KS, U.S.A., functioned as a reference electrode (measured as -0.006 V vs saturated calomel electrode, SCE, [Hg/Hg<sub>2</sub>Cl<sub>2</sub>, KCl (saturated)], which is equivalent to +0.235 V vs SHE). A platinum foil from Goodfellow, Cambridge, U.K., acted as a counter electrode. All experiments were conducted under a hydrogen or nitrogen atmosphere. All electrochemical measurements were thermostated at  $25 \pm 0.5$  °C.

An in-house built low noise, highly stabilized (1 kHz bandwidth) classic adder potentiostat was employed to control the potential and impact current measurements.<sup>1</sup> The computer interface was connected *via* an USB to an NI USB-6003 data acquisition (DAQ) device. The DAQ was purchased from National Instruments, Austin, TX, U.S.A. and was controlled by Python 3.5 (Canopy from Enthought, Austin, TX, U.S.A). The working electrode was running to ground where a low-noise current amplifier LCA-200-10G or LCA-4K-1G from FEMTO, Messtechnik GmbH, Germany was used to measure currents. The incoming analogue signal was oversampled and digitized by the DAQ device at a stream rate of 100 kHz, and the digitised signal was subsequently filtered at a bandwidth of 100 Hz.

## S2: TEM and UV-Vis Characterisation

An important factor to consider is the extent to which these particles may be agglomerated in the electrochemical cell, plausibly encouraged by the presence of millimolar electrolyte concentrations.<sup>2-3</sup> The stability of the nanoparticle suspension in bulk solution may be readily monitored *via* UV-vis spectroscopy. SI Figure S1 (Section 2) presents the variation of the platinum plasmon peak (*ca.* 300 nm)<sup>4</sup> as a function of time in the presence of 20 mM KOH and with hydrogen in solution. With the inset of Figure S1 showing the UV-vis absorbance measured at the peak (295 nm) against the experimental time under both hydrogen and nitrogen conditions. On the basis of these ensemble measurements it is concluded that the nanoparticle sol is metastable. Consequently, in order to *minimize* the influence of agglomeration upon the results all experiments were restricted to being performed in the first 30 minutes after the electrolyte was added to the nanoparticle sol. The stock mesoporous PtNP samples were characterized *via* transmission electron microscopy (TEM) and ultraviolet–visible (UV-vis) spectroscopy.

### 1.3.1 TEM

TEM (JEOL JEM-3000F FEGTEM, 300 kV accelerating voltage) was performed using conventional bright field imaging to determine the size of mesoporous PtNPs. Samples were prepared by depositing a drop of the stock mesoporous PtNP suspension, with concentration  $3.3 \times 10^{13}$  particles L<sup>-1</sup> onto a carbon TEM grid coated with holey carbon film from Agar Scientific, Stansted, U.K. Air drying was allowed before any further examination. ImageJ software<sup>4</sup> developed at the National Institutes of Health, U.S.A., was used to analyze the TEM images. Example images are shown in Figure 1 a. Clearly defined mesoporous PtNPs consisting of an aggregation small particles were measured and both radii calculated. A total count of 86 mesoporous PtNPs gave a mean radius of  $23.1 \pm 2.1$  nm, close to the value of 25 nm provided by the manufacturer; 49 small particles were averaged to give a mean radius of  $2.0 \pm 0.3$  nm. The corresponding size distributions are presented in Figure 1 b. To clarify, in this paper, the “mesoporous PtNP” refers to the mesoporous 23.1 nm particle, and the “small particles” are the components of a mesoporous PtNP.

### 1.3.2 UV-Vis Spectroscopy

UV-vis (Shimadzu UV-1800 UV-vis spectrophotometer) measurements were conducted to evidence the stability of mesoporous PtNP colloids. The stock mesoporous PtNP suspension was diluted by a factor of 2 with ultrapure water to obtain absorbance in an analytically meaningful range. Both deuterium and halogen light sources were used, with the sample being scanned from 900 to 250 nm. A broad surface plasmon peak around 300 nm was recorded over 2 hours indicating the presence of mesoporous PtNPs.<sup>5</sup> Mesoporous PtNPs were stable in 20 mM KOH in the presence of H<sub>2</sub> within 30

minutes, as shown in Figure S1. The UV-vis plasmon adsorption peak decreased after 30 minutes, suggesting an agglomeration of the nanoparticles. In order to minimise the influence of agglomeration upon the results all experiments were restricted to being performed in the first 30 minutes after any electrolyte was added to the nanoparticle sol.

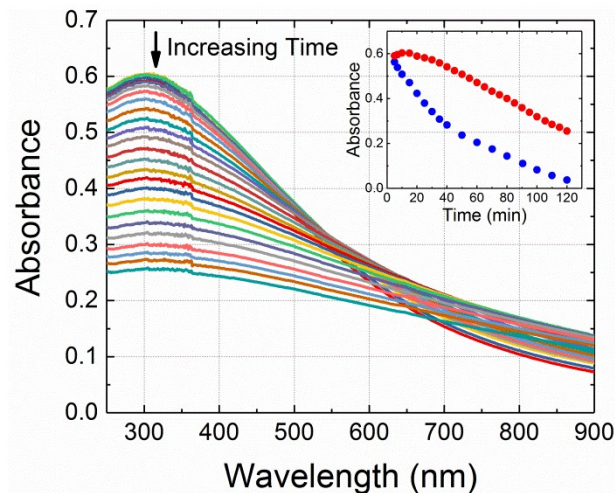


**Figure S1** UV-vis spectrum of the mesoporous PtNPs in 20 mM KOH with H<sub>2</sub>. Inlay: plot of the absorbance against the experimental time measured at a wavelength of 295 nm. Red circle and blue circle represent PtNPs in 20 mM KOH with H<sub>2</sub> and N<sub>2</sub>, respectively.

### S3: Underpotential Hydrogen Deposition ( $H_{\text{upd}}$ ) Reduction

Immersion of a gold microelectrode (10  $\mu\text{m}$  diameter) under potentiostatic control into an alkaline solution (20 mM KOH) containing mesoporous PtNPs (6.7 pM) results in the observation of small spikes in the measured time-current profile. Figure S2 depicts representative chronoamperograms where the gold working electrode has been held at a potential of -0.60 V (vs Ag/AgCl in 1M KCl) under nitrogen condition. Also plotted are zoomed versions of the current transient showing the individual spikes. The impact spikes are found to be  $0.2\pm 0.02$  pC in magnitude and correspond to the arrival of individual nanoparticle entities to the electrode, whence upon electrical contact with the electrified interface the nanoparticles are modified by the reduction of water to underpotential hydrogen deposition ( $H_{\text{upd}}$ ). The resulting spike gives a direct measure of the internal structure of the individual particle entities. By comparing the nanoparticle sizes obtained from the TEM, 70-80% nanoimpacts observed in experiments are estimated to be due to the arrival of single nanoparticles (see Figure 3, main text).

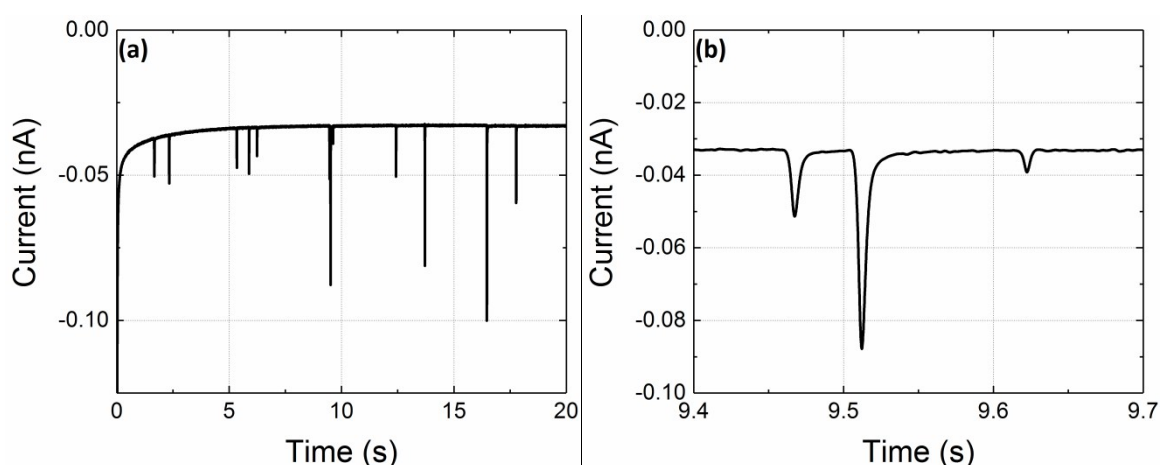
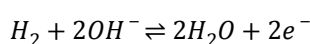


**Figure S2** (a) A chronoamperogram of 6.7 pM mesoporous PtNPs in 20 mM KOH at an Au microelectrode with an applied potential of -0.60 V (vs Ag/AgCl in 1 M KCl). (b) Zoomed in plots of (a). The electrolyte is 20 mM KOH saturated with  $N_2$ .

#### S4: Underpotential Hydrogen Deposition ( $H_{\text{upd}}$ ) Oxidation

First micro arrays of nanoparticles are investigated; a gold microelectrode (radius = 5  $\mu\text{m}$ ) was submerged into a PtNP suspension (6.7 pM) containing 20 mM KOH and saturated with hydrogen. Cyclic voltammetry was performed from -1.0 to 1.0 V vs Ag/AgCl in 1 M KCl (Figure S3). In the presence of hydrogen ( $[\text{H}_2]_{\text{sat}} = 0.73 \text{ mM}$ )<sup>6</sup> the voltammetric response of the gold electrode, modified in-situ by the solution-phase nanoparticles, shows a clear voltammetric peak at -0.5 V. The magnitude of this wave increases with exposure time of the electrode to the nanoparticle sol and is associated with the catalytic oxidation of hydrogen at the surface of the adsorbed PtNPs. In the absence of the PtNPs no oxidative wave is observed. Overall under alkali conditions the hydrogen oxidation is:



Further, at platinum surfaces - as is seen in Figure S3 - the HOR becomes inhibited at high overpotentials, this reportedly arises due to specific anion adsorption.<sup>7</sup> We also note the voltammetric feature shown in Figure S3 with a forward peak at +0.37 V and a reverse peak at 0.09 V which is associated with the oxidation of the micro gold electrode substrate and is seen in the absence of PtNPs.

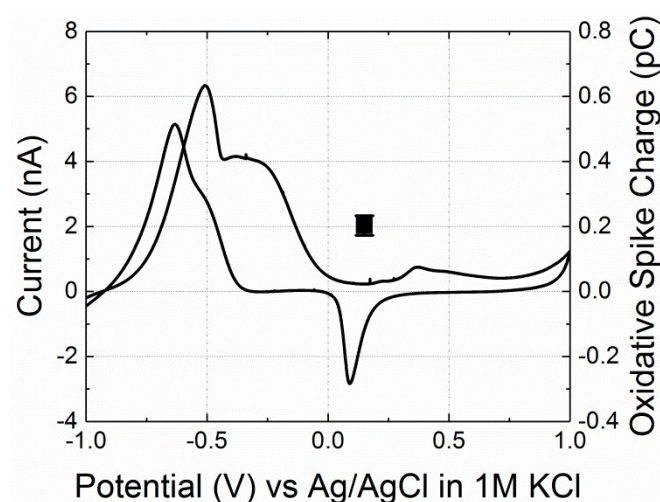


**Figure S3** Cyclic voltammograms for  $H_{\text{upd}}$  oxidation (solid line) on an Au microelectrode with a random array of adsorbed mesoporous PtNPs (CV of scan rate 200  $\text{mVs}^{-1}$ ; nanoparticle of radius 23.1 nm, electrode of radius 5  $\mu\text{m}$ ). Overlaid is the current response of individual mesoporous PtNPs at applied potential of +0.15 V (black square) vs Ag/AgCl in 1 M KCl (measured from the time current transients, 200 ms after the nanoparticle arrival). The electrolyte is 20 mM KOH saturated with  $\text{N}_2$ .

Second the responses of individual particles impacting at the gold substrate are considered; Upon impact of the nanoparticles to an electrode potentiostated above 0.0 V vs Ag/AgCl - such that the oxidation of solution phase hydrogen is inhibited - oxidative spikes in current are observed, corresponding to the removal of the adsorbed  $H_{\text{upd}}$  layer from the platinum surface. Therefore to study the  $H_{\text{upd}}$  oxidation a potential of +0.15 V (vs Ag/AgCl in 1 M KCl) is selected for chronoamperometry (*vide infra*) to avoid any influence caused by the hydrogen oxidation occurred at more negative potentials.

A gold microelectrode (10  $\mu\text{m}$  diameter) is immersed under potentiostatic control into an alkaline solution (20 mM KOH) containing mesoporous PtNPs (6.7 pM), resulting in the observation of small spikes in the measured time-current profile. Figure S4 depicts representative chronoamperograms where the gold working electrode has been held at a potential of +0.15 V (vs Ag/AgCl in 1M KCl) under hydrogen condition. The size of spikes detected varies as the PtNPs have a size distribution. Also plotted are zoomed versions of the current transient showing the individual spikes.

For chronoamperograms conducted at +0.15 V the magnitude of these current spikes are determined (overlay in Figure S3) to give a mean value of *ca.* 0.2 pC. These resulting spikes correspond to the arrival of individual nanoparticle entities to the electrode, whence upon electrical contact with the electrified interface the nanoparticles are modified by the oxidation of underpotential hydrogen deposition ( $H_{\text{upd}}$ ) to water, and therefore give a direct measure of the internal structure of the individual particle entities. To note these average oxidative charges passed (*ca.* 0.2 pC) are directly comparable in magnitude to those found reductively (see main text).

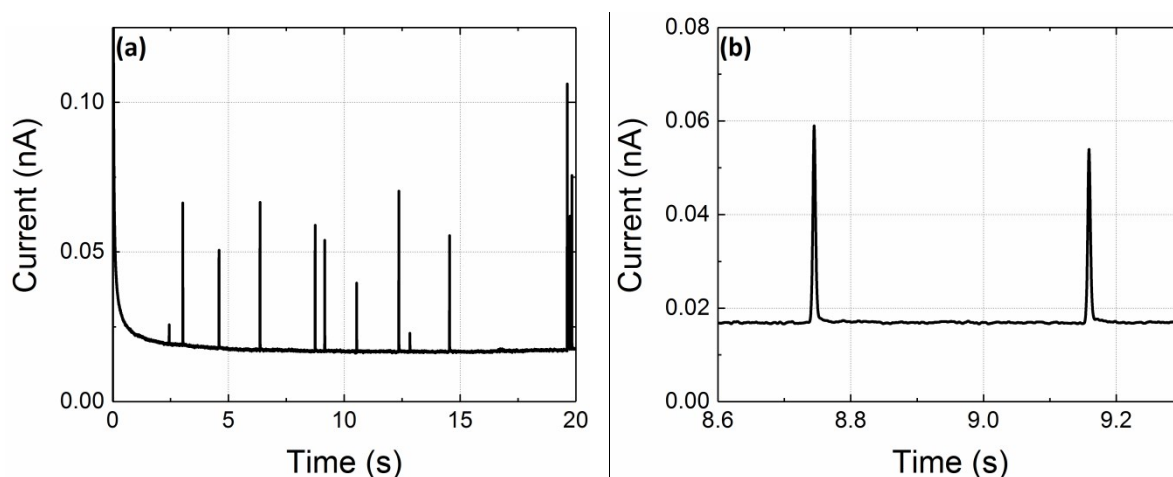


**Figure S4** (a) A chronoamperogram of 6.7 pM mesoporous PtNPs in 20 mM KOH at an Au microelectrode with an applied potential of +0.15 V (vs Ag/AgCl in 1 M KCl). (b) Zoomed in plots of (a). The electrolyte is 20 mM KOH saturated with  $H_2$ .



## S5: Mesoporous Platinum Nanoparticle Electroactive Surface Area Measurements

As a result of the mesoporous structure of the nanoparticles, to what extent is the internal structures of this material electrochemically accessible? Table S1 presents a summary of the charge measured *via* the nano-impact technique utilising  $H_{\text{upd}}$  - both reductive and oxidative - and from the literature as measured *via* platinum oxidation and nitro group reduction. In all cases presented in Table S1 these measurements have been made using the same mesoporous platinum nanoparticles and performed in the presence of millimolar electrolyte concentrations. Moreover all of these processes are surface reactions and the magnitude of the charge passed per event is proportional to the particles electroactive area. The reported areas per redox active group have been calculated on the assumption that the total surface area of a single particle is  $5.7 \times 10^{-2} \mu\text{m}^2$  (for  $H_{\text{upd}}$  reduction and oxidation) or  $6.7 \times 10^{-2} \mu\text{m}^2$  (for nitro group reduction and platinum oxidation). This discrepancy of surface area results from the slightly difference size of PtNP aggregates based on the TEM measurement. For comparison the surface coverage of NTP (4-nitrothiophenol) on a gold surface has been previously reported to be  $48.3 \text{ \AA}^2$ <sup>8</sup> and the area per platinum atom on a polycrystalline platinum surface is approximately  $7.6 \text{ \AA}^2$  (as calculated on the basis of  $H_{\text{upd}}$  signal of  $210 \mu\text{C cm}^{-2}$  and assuming one hydrogen atom per platinum). The  $H_{\text{upd}}$  area calculated from experimental results is smaller than the literature value. This is because in the calculation we assume one spike correlates to one single nanoparticle impact and do not account for agglomeration. From the cumulative frequency plot (Figure 3, main text), we can see a 20-30% agglomeration of the nanoparticles in the experiment time scale. Consequently, the areas per redox active group as measured on a *per particle* basis strongly indicate that the *entire* nanoparticle surface is electroactive. In the case of the  $H_{\text{upd}}$  measurements, the influence of particle agglomeration on the reported effective area per redox active group is considered in the main text.

**Table S1** Surface area measurements per redox active groups (RAG): nitro group reduction, platinum oxidation,  $H_{\text{upd}}$  reduction and oxidation (at  $-0.60$  and  $+0.15$  V vs Ag/AgCl in 1 M KCl), area per RAG is calculated on the basis of the surface area of one mesoporous PtNP obtained from TEM.

	Average Charge per PtNP impact (pC)	Number of Electron Transfer per RAG	Area per RAG ( $\text{A}^2$ )
Nitro Group Reduction <sup>9</sup>	0.094	4	45.5
Platinum Oxidation <sup>10</sup>	0.15	1.1	7.8
$H_{\text{upd}}$ Reduction	0.21	1	4.4
$H_{\text{upd}}$ Oxidation	0.20	1	4.6

## S6: Hydrogen Evolution Reaction (HER) under Nitrogen or Hydrogen Condition

First a gold microelectrode (10  $\mu\text{m}$  diameter) was immersed into an alkaline solution (20 mM KOH) under nitrogen condition. Hydrogen evolution reaction (HER) signal is observed at potentials negative to -1.20 V vs Ag/AgCl in 1 M KCl (shown in Figure S5). To further study the HER on the platinum surface a potential of -1.30 V (vs Ag/AgCl in 1 M KCl) is selected for chronoamperometry (*vide infra*) because at this potential no significant hydrogen evolution occurs on the bare gold substrate based on Figure S5. However HER is significantly observed in Figure 2 (main text) on PtNP surfaces. This 0.3 V difference in the onset of hydrogen evolution potentials in Figures 2 and S5 is due to the presence of platinum nanoparticles on the gold electrode surface in the voltammogram presented in Figure 2 of the main text.

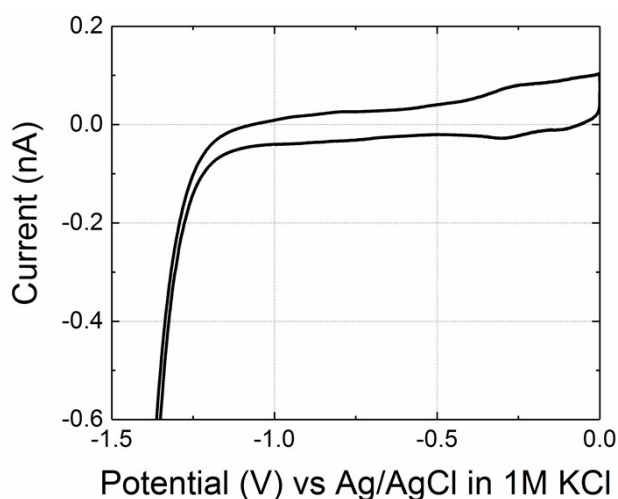


**Figure S5** A cyclic voltammogram for HER on an Au microelectrode (CV of scan rate 200  $\text{mVs}^{-1}$ , electrode of radius 5  $\mu\text{m}$ ). The electrolyte is 20 mM KOH saturated with  $\text{N}_2$ .

Second immersion of the gold working electrode under potentiostatic control into an alkaline solution (20 mM KOH) containing mesoporous PtNPs (6.7 pM) results in the observation of small steps in the measured time-current profile. Figure S6 and S7 depict representative chronoamperograms where the gold electrode has been held at a potential of -1.30 V (vs Ag/AgCl in 1M KCl) under nitrogen and hydrogen conditions, respectively. Also plotted are zoomed versions of the current transient showing the individual steps in current. The current steps are found to be around a few picoampere in magnitude and correspond to the arrival of individual nanoparticle entities to the electrode, whence upon electrical contact with the potentiostatted interface the nanoparticles serve to catalyse the reduction of water to hydrogen. The resulting step gives a direct measure of the reaction rate occurring at the individual particle entities. To note, under nitrogen condition (Figure S6) an initial peak in current prior to the reductive step is observed, which can be directly compared to Figure S7

under hydrogen condition. This initial peak appeared in saturated nitrogen gives a direct measure of the internal structure of the individual particle entities.

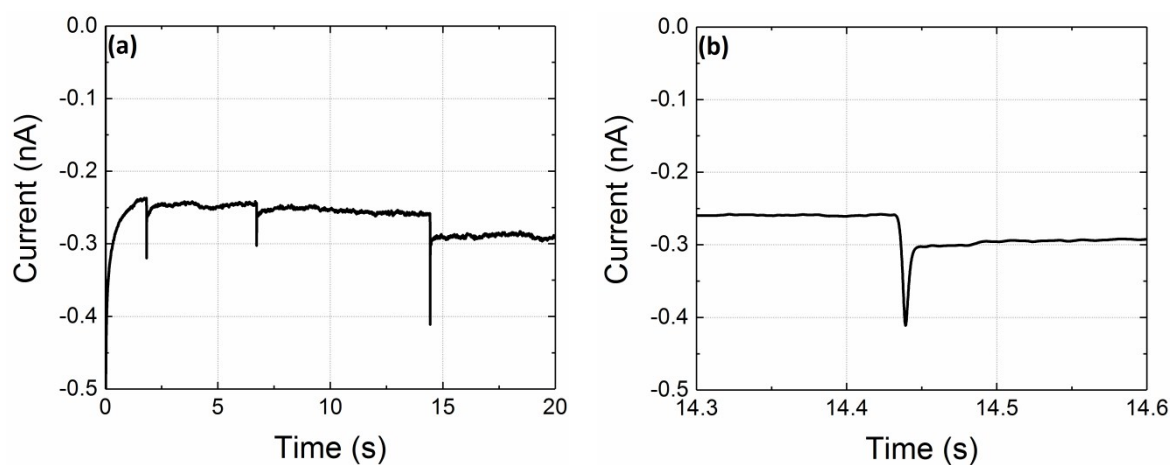


**Figure S6** (a) A chronoamperogram of 6.7 pM mesoporous PtNPs in 20 mM KOH at an Au microelectrode with an applied potential of -1.30 V (vs Ag/AgCl in 1 M KCl). (b) Zoomed in plots of (a). The electrolyte is 20 mM KOH saturated with  $N_2$ .

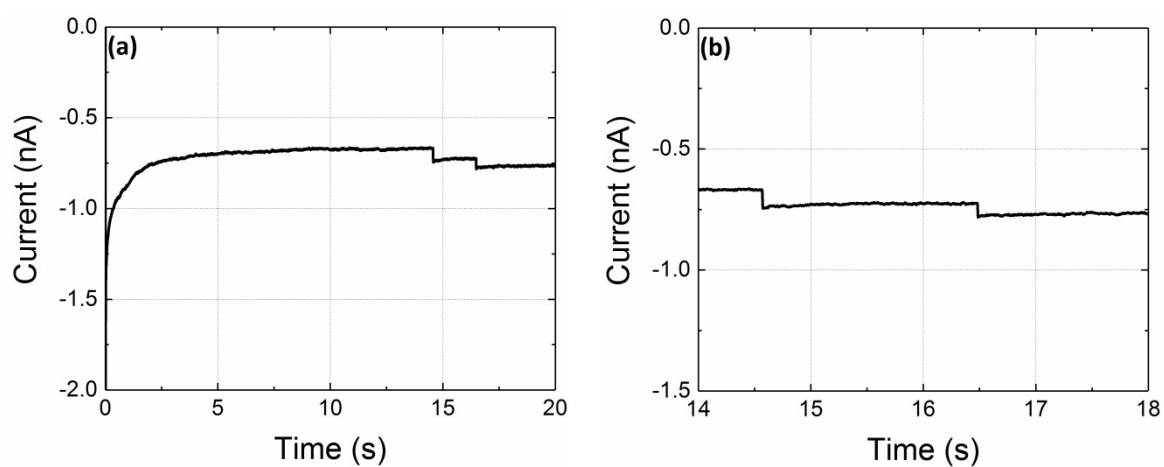


**Figure S7** (a) A chronoamperogram of 6.7 pM mesoporous PtNPs in 20 mM KOH at an Au microelectrode with an applied potential of -1.30 V (vs Ag/AgCl in 1 M KCl). (b) Zoomed in plots of (a). The electrolyte is 20 mM KOH saturated with  $H_2$ .

### S7: Current Density of Hydrogen Evolution Reaction (HER) on Platinum Bulk

First a platinum microelectrode (10  $\mu\text{m}$  diameter) was immersed into an acidic solution (1 mM  $\text{HClO}_4$  and 19 mM  $\text{KClO}_4$ ) under nitrogen.  $\text{H}_{\text{upd}}$  reduction and oxidation signals are observed at -0.20 V vs Ag/AgCl in 3.4 M KCl (shown in Figure S8). The charge of  $\text{H}_{\text{upd}}$  on platinum bulk was determined to be  $5.0 \times 10^{-10}$  C by integrating the current underneath the cyclic voltammogram (-0.34 to -0.00 V). This charge value dividing by the geometric area of the electrode gives a charge density of  $\sim 6.4 \text{ C m}^{-2}$ . By comparing with the literature value, taking the monolayer coverage of  $\text{H}_{\text{upd}}$  on a platinum surface ( $2.1 \text{ C m}^{-2}$ )<sup>11</sup>, the electrode surface roughness of the polycrystalline platinum estimated to be factor of 3.0. Therefore the electroactive area of the electrode is triple that of the geometric area.

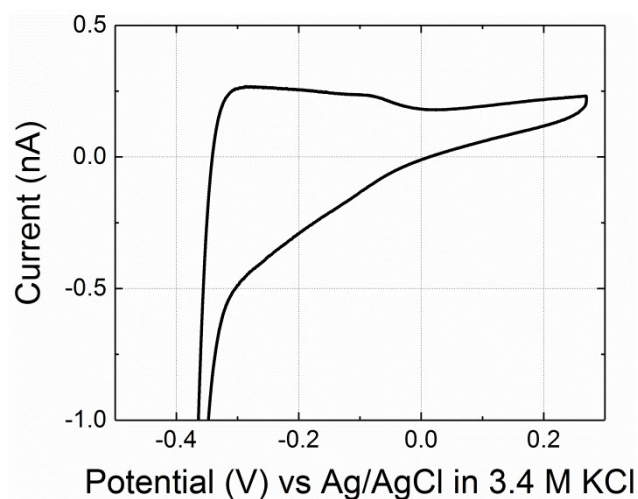


**Figure S8** A cyclic voltammogram for  $\text{H}_{\text{upd}}$  reduction on a Pt microelectrode (CV of scan rate  $200 \text{ mVs}^{-1}$ , electrode of radius  $5 \mu\text{m}$ ). The electrolyte is 1 mM  $\text{HClO}_4$  and 19 mM  $\text{KClO}_4$  saturated with  $\text{N}_2$ .

Second a platinum microelectrode (10  $\mu\text{m}$  diameter) was immersed into an alkaline solution (20 mM KOH) under nitrogen condition. Hydrogen evolution reaction (HER) signal is observed at potentials negative to -0.90 V vs Ag/AgCl in 3.4 M KCl (shown in Figure S9). The current density of hydrogen evolution reaction (HER) on platinum bulk at -1.33 V (vs Ag/AgCl in 3.4 M KCl) can be calculated using the current measured at this potential (-83 nA) divided by the electroactive area of the electrode, giving a value of  $\sim 352 \text{ A m}^{-2}$ .

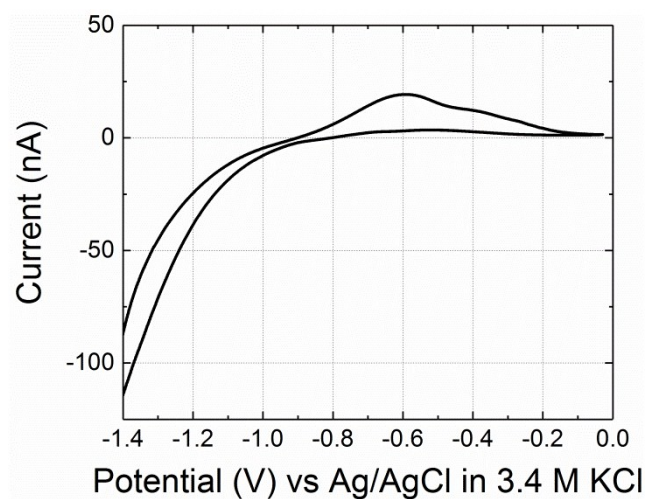


**Figure S9** A cyclic voltammogram for HER on a Pt microelectrode (CV of scan rate  $200 \text{ mVs}^{-1}$ , electrode of radius  $5 \mu\text{m}$ ). The electrolyte is  $20 \text{ mM KOH}$  saturated with  $\text{N}_2$ .

## Reference

1. Batchelor-McAuley, C.; Ellison, J.; Tschulik, K.; Hurst, P. L.; Boldt, R.; Compton, R. G., In Situ Nanoparticle Sizing with Zeptomole Sensitivity. *Analyst* **2015**, *140*, 5048-5054.
2. Kleijn, S. E. F.; Serrano-Bou, B.; Yanson, A. I.; Koper, M. T. M., Influence of Hydrazine-Induced Aggregation on the Electrochemical Detection of Platinum Nanoparticles. *Langmuir* **2013**, *29*, 2054-2064.
3. Furlong, D. N.; Launikonis, A.; Sasse, W. H. F.; Sanders, J. V., Colloidal Platinum Sols. Preparation, Characterization and Stability Towards Salt. *J. Chem. Soc., Faraday Trans. 1* **1984**, *80*, 571-588.
4. Broeke, J.; Perez, J. M. M.; Pascau, J., *Image Processing with Imagej*; Packt Publishing, 2015.
5. Creighton, J. A.; Eadon, D. G., Ultraviolet-Visible Absorption Spectra of the Colloidal Metallic Elements. *J. Chem. Soc., Faraday Trans.* **1991**, *87*, 3881-3891.
6. Wilhelm, E.; Battino, R.; Wilcock, R. J., Low-Pressure Solubility of Gases in Liquid Water. *Chem. Rev.* **1977**, *77*, 219-262.
7. Zalitis, C. M.; Kucernak, A. R.; Sharman, J.; Wright, E., Design Principles for Platinum Nanoparticles Catalysing Electrochemical Hydrogen Evolution and Oxidation Reactions: Edges Are Much More Active Than Facets. *J. Mater. Chem. A* **2017**, *5*, 23328-23338.
8. Nielsen, J. U.; Esplandiu, M. J.; Kolb, D. M., 4-Nitrothiophenol SAM on Au(111) Investigated by in Situ STM, Electrochemistry, and XPS. *Langmuir* **2001**, *17*, 3454-3459.
9. Jiao, X.; Sokolov, S. V.; Tanner, E. E. L.; Young, N. P.; Compton, R. G., Exploring Nanoparticle Porosity Using Nano-Impacts: Platinum Nanoparticle Aggregates. *Phys. Chem. Chem. Phys.* **2017**, *19*, 64-68.
10. Jiao, X.; Tanner, E. E. L.; Sokolov, S. V.; Palgrave, R. G.; Young, N. P.; Compton, R. G., Understanding Nanoparticle Porosity via Nanoimpacts and XPS: Electro-Oxidation of Platinum Nanoparticle Aggregates. *Phys. Chem. Chem. Phys.* **2017**, *19*, 13547-13552.
11. Trasatti, S.; Petrii, O. A., Real Surface Area Measurements in Electrochemistry. *Pure Appl. Chem.* **1991**, *63*, 711-734.